Journal of Vibration and Control
http://jvc.sagepub.com/

Free vibration of tapered beams and plates based on unified beam theory

Syed Muhammad Ibrahim, Saleh H Alsayed, Husain Abbas, Erasmo Carrera, Yousef A Al-Salloum and Tarek H Almusallam

Journal of Vibration and Control published online 26 June 2013
DOI: 10.1177/1077546312473766

The online version of this article can be found at:
http://jvc.sagepub.com/content/early/2013/06/26/1077546312473766

Published by:
SAGE
http://www.sagepublications.com

Additional services and information for *Journal of Vibration and Control* can be found at:

Email Alerts: http://jvc.sagepub.com/cgi/alerts

Subscriptions: http://jvc.sagepub.com/subscriptions

Reprints: http://www.sagepub.com/journalsReprints.nav

Permissions: http://www.sagepub.com/journalsPermissions.nav

>> OnlineFirst Version of Record - Jun 26, 2013

What is This?

Downloaded from jvc.sagepub.com by Erasmo Carrera on August 26, 2014

Article

Journal of Vibration and Control
0(0) 1–14
© The Author(s) 2013
Reprints and permissions:
sagepub.co.uk/journalsPermissions.nav
DOI: 10.1177/1077546312473766
jvc.sagepub.com
SAGE

Free vibration of tapered beams and plates based on unified beam theory

Syed Muhammad Ibrahim[1], Saleh H Alsayed[1], Husain Abbas[1], Erasmo Carrera[2], Yousef A Al-Salloum[1] and Tarek H Almusallam[1]

Abstract

In this paper, accurate frequency solutions of tapered vibrating beams and plates using a simple and efficient displacement based unified beam theory in lieu of computationally expensive and rather complex two-dimensional plate theories are presented. The results are given in the form of Euler-Bernoulli/Timoshenko to quasi three-dimensional (3D) solutions. Lower frequency bending and axial modes, as well as torsional and biaxial bending modes corresponding to higher frequency values, are predicted which are in very good agreement with 3D finite element results as well as the published literature. The effects of different parameters like taper ratio, thickness and beam/plate-aspect ratios on the vibration frequencies of tapered structures are studied. It can be seen that due to taper, bending vibration modes become asymmetric along the longitudinal axis of the structure. Further, it can also be noticed that the vibration behavior of thicker beams and plates is characterized by the appearance of a significant number of axial modes at lower frequency values as compared to that of relatively thinner beams/plates.

Keywords

Higher order theory, tapered beams, tapered plates, unified beam formulation, vibration

1. Introduction

Thin-walled beam and plate structures are one of the most widely used load carrying members in structural engineering applications. Theoretical as well as experimental studies of these structures with variable geometric parameters have attracted the interest of researchers not only because of the need for rational and economic profiling of structures but also due to specific shape requirements at certain locations. This can be achieved and complemented by accurately evaluating their design parameters, like natural frequencies for structures which are subjected to a dynamic environment during their service life.

The vast literature that exists on the vibration analysis of tapered beams and plates deals mainly with lower modes of thin sections. Many recent analyses based on theories taking into account constant and uniform transverse shear deformation of tapered and non-classical beams have also been carried out (e.g. Auciello and Ercolano, 2004; Piovan et al., 2008; Attarnejad et al., 2010; Hajianmaleki and Qatu, 2012). Free vibration studies of plates with constant thickness have also been carried out extensively using first order (Dawe and Wang, 1994; Liew et al., 1998; Shufrin and Eisenberger, 2005) and higher order theories (Reddy and Phan, 1985; Doong, 1987; Hanna and Leissa, 1994; Matsunga, 1994). However, studies pertaining to vibration of tapered plates considering first order and higher order theories are limited. Mikami and Yoshimura (1984) studied free vibration characteristics of linearly tapered rectangular plates using the

[1]Specialty Units for Safety and Preservation of Structures, Department of Civil Engineering, King Saud University, Saudi Arabia
[2]Department of Mechanical and Aerospace Engineering, Politecnico di Torino, Torino, Italy

Received: 3 June 2012; accepted: 8 December 2012

Corresponding author:
H Abbas, Specialty Units for Safety and Preservation of Structures, Department of Civil Engineering, King Saud University, PO Box 800, Riyadh 11421, Saudi Arabia.
Email: abbas_husain@hotmail.com

Downloaded from jvc.sagepub.com by Erasmo Carrera on August 26, 2014

collocation method with orthogonal polynomials based on first order shear deformation theory (FSDT). Based on FSDT, Mizusawa (1993) investigated the vibration characteristics of plates with variable thickness using the spline strip method. Finite difference technique has been employed by Al-Kaabi and Aksu (1987, 1988, 1990) for the analysis of linearly, bilinearly and parabolically tapered Reisner-Mindlin plates. Cheung and Zhou (2003) presented solutions for the natural frequencies of tapered plates with different boundary conditions using the finite strip method. The differential quadrature method (DQM) in conjunction with FSDT was employed by Malekzadeh and Karami (2004) for the vibration analysis of non-uniform thick plates on elastic foundations. Quintana and Nallim (2010) used variational approach based on Reissner–Mindlin plate theory to analyze the free vibration of shear deformable polygonal plates with variable thickness. Manna (2012) studied the free vibration of tapered plates using a high precision triangular finite element. Gupta and Sharma (2011, 2012) studied the thermal vibration behavior of symmetric trapezoidal plates using the Rayleigh Ritz method. Only the frequencies corresponding to the first two bending modes of vibration were evaluated for the trapezoidal plate for different values of thermal gradient, taper constant and aspect ratio. Employing extended Kantorovich method (Kerr, 1969), Shufrin and Eisenberger (2006) obtained frequency parameters for thick tapered plates using first and higher order shear deformation theories. To the best of the authors' knowledge, no studies are available for the solution of free vibration of rectangular plates and beams with variable thickness dealing with bending, torsional as well as axial modes in unified manner. Further, in most of the studies, the investigations were limited to the vibration behavior of tapered plates considering only the first few lower frequency modes.

The objective of the present work is to obtain accurate frequency solutions of tapered vibrating beams and plates using a simple and efficient displacement based unified beam theory (Carrera et al., 2011) in lieu of computationally expensive and rather complex two-dimensional (2D) plate theory. The results are presented in the form of Euler-Bernoulli beam theory (EBBT) solutions to quasi 3D solutions. Modes like bending, torsional, biaxial bending as well different kinds of inplane modes are captured which are in very good agreement with three-dimensional (3D) finite element results as well as the published literature. The effects of different parameters like taper ratio, thickness and beam/plate-aspect ratios on the vibration frequencies of tapered structures are studied. It can be seen that due to taper, bending vibration modes become asymmetric along the longitudinal axis of the structure. Further, it can also be noticed that the vibration behavior of thicker beams and plates is characterized by the appearance of a significant number of axial modes at lower frequency values as compared to that of relatively thinner beams/plates.

2. Formulation

2.1. Preliminaries

Geometry and the chosen coordinate system are given in Figure 1. y- axis is considered as the longitudinal axis and x- and z- axes describes the cross-section represented by Ω. The beam boundaries over y are $0 \le y \le L_y$. The displacement vector, representing the three displacement components, can be written as:

$$\left[\mathbf{u}_{(x,y,z)}\right] = \left[\, u_x \quad u_y \quad u_z \,\right]^T. \tag{1}$$

Stress and strain components for any point P_Ω (x, y, z) which lie on the reference surface Ω can be given as (Carrera et al., 2011):

$$\left[\boldsymbol{\sigma}_p\right] = \left[\, \sigma_{zz} \quad \sigma_{xx} \quad \sigma_{zx} \,\right]^T, \quad \left[\boldsymbol{\sigma}_n\right] = \left[\, \sigma_{zy} \quad \sigma_{xy} \quad \sigma_{yy} \,\right]^T, \tag{2}$$

$$\left[\boldsymbol{\varepsilon}_p\right] = \left[\, \varepsilon_{zz} \quad \varepsilon_{xx} \quad \varepsilon_{zx} \,\right]^T, \quad \left[\boldsymbol{\varepsilon}_n\right] = \left[\, \varepsilon_{zy} \quad \varepsilon_{xy} \quad \varepsilon_{yy} \,\right]^T, \tag{3}$$

The subscript n stands for terms lying on the cross-section, while p represents the terms lying on reference planes which are orthogonal to Ω.

Similarly, strain – displacement relations can be written as:

$$\left[\boldsymbol{\varepsilon}_p\right] = \left[\mathbf{D}_p\right]\left[\mathbf{u}\right], \; \left[\boldsymbol{\varepsilon}_n\right] = \left[\mathbf{D}_n\right]\left[\mathbf{u}\right] = \left(\left[\mathbf{D}_{n\Omega}\right] + \left[\mathbf{D}_{ny}\right]\right)\left[\mathbf{u}\right], \tag{4}$$

and

$$\left[\mathbf{D}_p\right] = \begin{bmatrix} 0 & 0 & D,z \\ D,x & 0 & 0 \\ D,z & 0 & D,x \end{bmatrix}, \quad \left[\mathbf{D}_{n\Omega}\right] = \begin{bmatrix} 0 & 0 & 0 \\ 0 & D,x & 0 \\ 0 & D,z & 0 \end{bmatrix},$$
$$\left[\mathbf{D}_{ny}\right] = \begin{bmatrix} 0 & D,y & 0 \\ D,y & 0 & 0 \\ 0 & 0 & D,y \end{bmatrix}, \tag{5}$$

where, D,x, D,y and D,z are partial differential operators with respect to x, y and z respectively.

Downloaded from jvc.sagepub.com by Erasmo Carrera on August 26, 2014

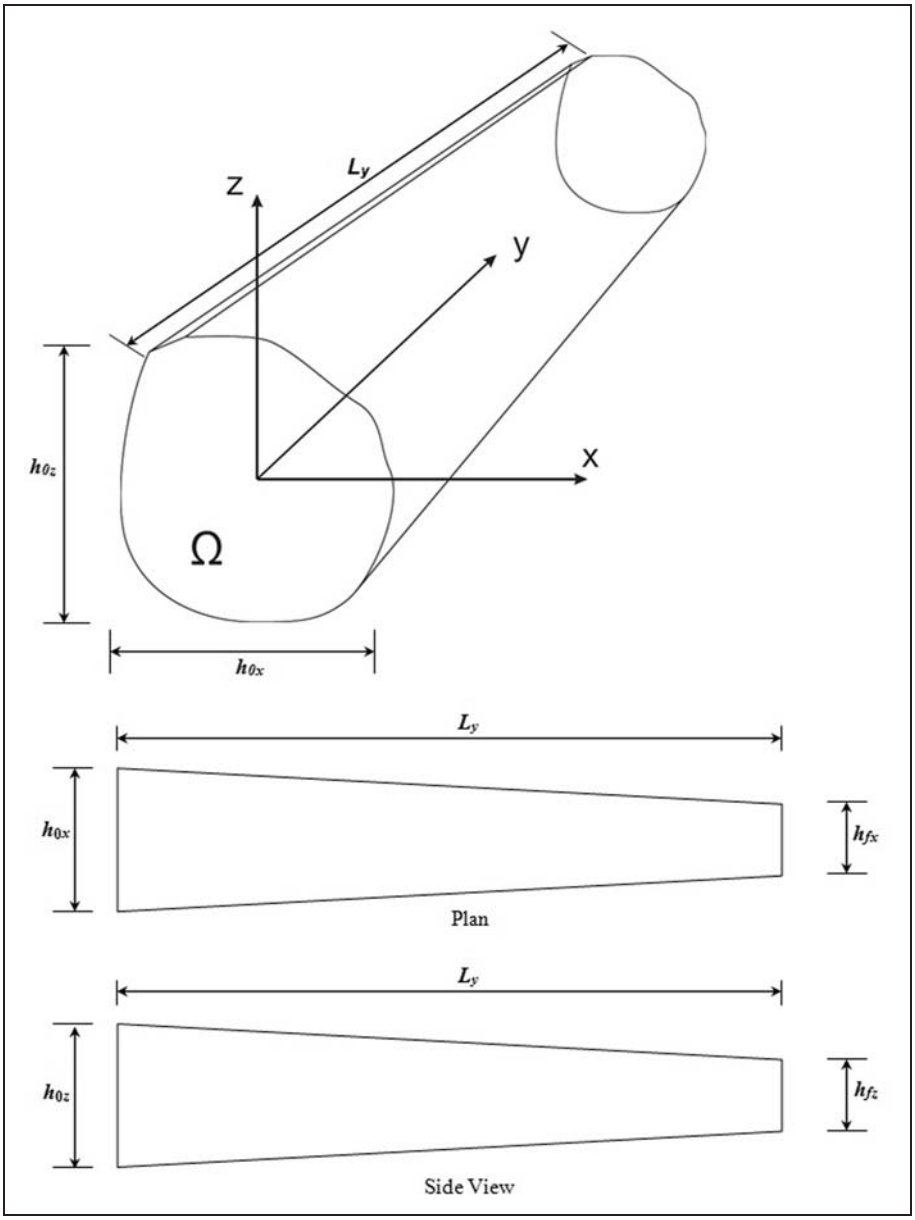

Figure 1. Geometry and coordinate system of tapered beam.

Material behavior can be assigned by exploiting Hooke's law and rewriting the stress – strain relations in terms of material constants as:

$$[\boldsymbol{\sigma}] = \begin{bmatrix} [\boldsymbol{\sigma}_p] \\ [\boldsymbol{\sigma}_n] \end{bmatrix} = \left[\tilde{\mathbf{C}}\right][\boldsymbol{\varepsilon}] \tag{6}$$

where,

$$\begin{aligned} [\boldsymbol{\sigma}_p] &= \left[\tilde{\mathbf{C}}_{pp}\right][\boldsymbol{\varepsilon}_p] + \left[\tilde{\mathbf{C}}_{pn}\right][\boldsymbol{\varepsilon}_n], \\ [\boldsymbol{\sigma}_n] &= \left[\tilde{\mathbf{C}}_{np}\right][\boldsymbol{\varepsilon}_p] + \left[\tilde{\mathbf{C}}_{nn}\right][\boldsymbol{\varepsilon}_n], \end{aligned} \tag{7}$$

and

$$\begin{aligned} \left[\tilde{\mathbf{C}}_{pp}\right] &= \begin{bmatrix} \tilde{C}_{11} & \tilde{C}_{12} & 0 \\ \tilde{C}_{12} & \tilde{C}_{22} & 0 \\ 0 & 0 & \tilde{C}_{66} \end{bmatrix}, \\ \left[\tilde{\mathbf{C}}_{nn}\right] &= \begin{bmatrix} \tilde{C}_{55} & 0 & 0 \\ 0 & \tilde{C}_{44} & 0 \\ 0 & 0 & \tilde{C}_{33} \end{bmatrix}, \\ \left[\tilde{\mathbf{C}}_{pn}\right] &= \left[\tilde{\mathbf{C}}_{np}^T\right] = \begin{bmatrix} 0 & 0 & \tilde{C}_{13} \\ 0 & 0 & \tilde{C}_{23} \\ 0 & 0 & 0 \end{bmatrix}. \end{aligned} \tag{8}$$

Downloaded from jvc.sagepub.com by Erasmo Carrera on August 26, 2014

Relations for material constants can be seen in Tsai (1988). It is important to mention here that $\left[\mathbf{D}_p\right]$, $[\mathbf{D}_{n\Omega}]$ and $\left[\mathbf{D}_{ny}\right]$ are 3×3 arrays of differential operators and $[\tilde{\mathbf{C}}_{pp}], [\tilde{\mathbf{C}}_{nn}], [\tilde{\mathbf{C}}_{pn}], [\tilde{\mathbf{C}}_{np}]$ have 3×3 stiffness components.

2.2. Unified theory

Now, in the displacement based formulation, the related displacement field is assumed as an expansion in terms of generic functions and can be written in compact form as:

$$[\mathbf{u}] = F_\tau[\mathbf{u}_\tau], \quad \tau = 1, N \tag{9}$$

where, $[\mathbf{u}_\tau]$ represents the introduced displacement variables of $P_\Omega(x, y, z)$ which lie on reference beam/plate surface Ω, F_τ are the introduced functions of coordinates x and z on the cross-section and N is a free parameter which represents the number of terms in expansion. According to the Einstein notation, the subscript τ indicates summation. The displacement field can be expanded by any polynomial function. In the present case, Maclaurin polynomial function, which uses as basis the 2D polynomials x^i, z^i is adopted. For example, considering expansion up to quadratic terms, the displacement field becomes:

$$\begin{aligned} u_x &= u_{x1} + xu_{x2} + zu_{x3} + x^2u_{x4} + xzu_{x5} + z^2u_{x6}, \\ u_y &= u_{y1} + xu_{y2} + zu_{y3} + x^2u_{y4} + xzu_{y5} + z^2u_{y6}, \\ u_z &= u_{z1} + xu_{z2} + zu_{z3} + x^2u_{z4} + xzu_{z5} + z^2u_{z6} \end{aligned} \tag{10}$$

From the above equations, Timoshenko beam theory (TBT) and EBBT can be obtained by imposing conditions on F_τ. The details can be seen in Carrera et al. (2011).

2.2.1. Finite element implementation. By introducing the shape function N_i and nodal displacement vector, $\mathbf{q}_{\tau i}$ ($\left[\mathbf{q}_{\tau i}\right] = \left[\, q_{u_{x\tau i}} \quad q_{u_{y\tau i}} \quad q_{u_{z\tau i}} \,\right]^T$), the displacement field can be written as:

$$[\mathbf{u}_\tau] = N_i F_\tau \left[\mathbf{q}_{\tau i}\right]. \tag{11}$$

Finite element is introduced along the longitudinal axis of the structure. In the present case, type B4 beam elements, i.e. elements with cubic approximation, are used along y-direction and details of which can be found in Bathe (1996). It is to be emphasized that beam expansion N, and the number of elements (and number of nodes per element) are totally free parameters and are not related to each other.

2.2.2. Variational equations. The governing equations variationally consistent with the present hypothesis can be obtained using principle of virtual displacement (PVD) as:

$$\delta\Pi_{\text{int}} = \int_V \left(\delta\left[\boldsymbol{\varepsilon}_p^T\right]\left[\boldsymbol{\sigma}_p\right] + \delta\left[\boldsymbol{\varepsilon}_n^T\right]\left[\boldsymbol{\sigma}_n\right]\right)\mathrm{d}V = \delta\Pi_{\text{ext}}, \tag{12}$$

where Π_{int} represents strain energy, and Π_{ext} is the work of the external loadings. δ stands for the virtual variation. In terms of the strain-displacement and material coefficients, virtual variation of the strain energy is rewritten using equations (4), (7) and (11), in a compact format in weak sense as:

$$\delta\Pi_{\text{int}} = \delta\left[\mathbf{q}_{\tau i}^T\right]\left[\mathbf{K}^{ij\tau s}\right]\left[\mathbf{q}_{sj}\right], \tag{13}$$

where $[\mathbf{K}^{ij\tau s}]$ is the stiffness matrix in the form of the fundamental nucleus. The first component of the fundamental nucleus can be written as:

$$\begin{aligned} K_{xx}^{ij\tau s} = {} & \tilde{C}_{22}\int_\Omega F_{\tau,x}F_{s,z}\,d\Omega\int_{L_y} N_i N_j\,dy \\ & + \tilde{C}_{66}\int_\Omega F_{\tau,z}F_{s,z}\,d\Omega\int_{L_y} N_i N_j\,dy \\ & + \tilde{C}_{44}\int_\Omega F_\tau F_s\,d\Omega\int_{L_y} N_{i,y} N_{j,y}\,dy \end{aligned} \tag{14}$$

The detailed expansion of the fundamental nucleus can be seen in Carrera and Petrolo (2012). It can be noted that the dimension of the fundamental nucleus is 3×3 array and can be used to any approximation of a 3D problem in an enlargement of initial 3×3 arrays of the 3D Hooke's law, e.g $\tilde{C}_{pp}\ldots$. etc. Surface integrals of F_τ and F_s are evaluated numerically by partitioning the integration area in a certain number of sub-domains. In the present case of tapered geometries, surface integrals are evaluated for each finite element.

2.2.3. Governing equations. The virtual variation of the work of the inertial loadings is:

$$\delta\Pi_{ine} = \int_V \rho\,[\ddot{\mathbf{u}}]\,[\delta\mathbf{u}]^T\mathrm{d}V, \tag{15}$$

where ρ is the mass density; $[\ddot{\mathbf{u}}]$ represents double derivate of displacement with respect to time. In terms of displacement vector and mass matrix $[\mathbf{M}^{ij\tau s}]$, equation can be rewritten as:

$$\delta\Pi_{ine} = \left[\delta\mathbf{q}_{\tau i}^T\right]\left[\mathbf{M}^{ij\tau s}\right]\left[\ddot{\mathbf{q}}_{sj}\right]. \tag{16}$$

Downloaded from jvc.sagepub.com by Erasmo Carrera on August 26, 2014

Similar to $[\mathbf{K}^{ij\tau s}]$, $[\mathbf{M}^{ij\tau s}]$ is also in the form of 3×3 fundamental nuclei and its nine components are:

$$M_{xx}^{ij\tau s} = M_{yy}^{ij\tau s} = M_{zz}^{ij\tau s} = \rho I_{\Omega}^{\tau s} I_{L_y}^{ij} \quad \text{and} \quad M_{xy}^{ij\tau s} = M_{xz}^{ij\tau s} = M_{yx}^{ij\tau s} = M_{yz}^{ij\tau s} = M_{zx}^{ij\tau s} = M_{zy}^{ij\tau s} = 0 \tag{17}$$

where, $I_{\Omega}^{\tau s} = \int_{\Omega} F_{\tau} F_s \, d\Omega$ and $I_{L_y}^{ij} = \int_{L_y} N_i N_j \, dy$.

Using the above equations, undamped free vibration problem can be solved as:

$$[\mathbf{M}][\ddot{\alpha}] + [\mathbf{K}][\boldsymbol{\alpha}] = [\mathbf{p}] \tag{18}$$

where $[\boldsymbol{\alpha}]$ is the vector of the nodal unknowns and $[\mathbf{p}]$ is the loadings vector. Natural frequency, ω_k can be obtained by the following eigenvalues problem:

$$\left(-\omega_k^2[\mathbf{M}] + [\mathbf{K}]\right)[\boldsymbol{\alpha}_k] = 0, \tag{19}$$

where $[\boldsymbol{\alpha}_k]$ is the kth eigen vector.

3. Numerical results

In this section, numerical results of square/rectangular and circular sections of beams tapered along the length as well as rectangular plates having tapered thickness obtained using the unified formulation are discussed. The results obtained using ANSYS as well as comparisons with published results in the case of plates are also presented. The cross-section of beams is represented by 4×4 SOLID45 elements whereas 40 SOLID45 elements are used in the longitudinal direction – thus making a total of 640 elements. The cross-section of plates is represented by 20×2 SOLID45 elements whereas 40 elements are used in the longitudinal direction – thus making a total of 1600 elements. On the basis of mesh sensitivity study, it is found that ten numbers of B4 beam elements are enough in the longitudinal direction for both beams and plates. The material properties considered are: Elastic Modulus, $E = 71.7$ GPa, Poisson ratio, $\nu = 0.3$ and density, $\rho = 2700\,\text{kg/m}^3$.

3.1. Beams

The first ten free vibration frequencies of clamped supported square cross-section beams for three different aspect ratios ($L_y/h_{0z} = 100$, 10 and 5; where L_y is length of beam and h_{0z} being the transverse dimension at $y = 0$) are taken up. For circular cross-section beams, results are presented for $L_y/h_{0z} = 10$. Two different tapering ratios (h_{fz}/h_{0z}; where h_{0z} and h_{fz} are thicknesses along z- axis of structure at $y = 0$ and $y = L_y$, respectively) of 0.5 and 0.25 are considered and compared with beams with constant cross-sections ($h_{fz}/h_{0z} = 1.0$).

3.1.1. Square cross-section beams ($L_y/h_{0z} = 100$). For the case of slender beams ($L_y/h_{0z} = 100$), first ten frequencies correspond to bending modes which occur in pairs for vibration in two transverse directions (e.g. modes 1 & 2, 3 & 4 represent the first and second bending modes in two transverse directions, respectively) as shown in Table 1. Due to its slenderness, results obtained using classical beam theories (EBBT and TBT) are accurate and no change is observed with further refinement (i.e. increase in the theory order N). It is to be noted that results for $N = 2$ are slightly on the higher side because of the artificial stiffness (Carrera and Brischetto, 2008). Also, the results are in complete agreement with ANSYS 3D results (total degrees-of-freedom, dof = 1024). Decrease in free vibration frequency for beams with $h_{fz}/h_{0z} = 0.5$ and 0.25 is about 27% and 43% respectively when compared with that of the corresponding modes of beam with constant cross-section. Note that the pairing order of higher modes is changed for the case of $h_{fz}/h_{0z} = 0.25$ (e.g. modes 5 & 7 and mode 6 & 9 represent third and fourth bending modes in two transverse directions, respectively). Vibration frequency for the modes in the un-tapered direction remains almost unaffected for both tapering ratios.

3.1.2. Square cross-section beams ($L_y/h_{0z} = 10$). Unlike the previous case, the first ten natural frequencies represent free vibration bending, torsional as well as axial modes which are marked in Table 1 (a – axial mode; t – torsional mode). EBBT overestimate the bending vibration frequencies. Torsional modes are completely missed by the classical theories whereas these are predicted using refined theory with expansion order as low as $N = 1$ albeit with slightly erroneous mode shapes. Further refined theory enables us to predict torsional as well as bending and axial modes adequately which are in good agreement with ANSYS 3D results. Considering the values of $N = 3$ as basis, there is a decrease of around 20–25% and 40% in frequencies of vibration modes in bending for $h_{fz}/h_{0z} = 0.5$ and 0.25, respectively with that of a beam with constant cross-section. For the first torsional modes, these values are 6% and 12%; whereas for the second, these are 9% and 15% of the corresponding beam with constant cross-section, respectively. Vibration frequency for axial mode remains almost unaffected for $h_{fz}/h_{0z} = 0.5$ whereas it gets reduced by around 3% for $h_{fz}/h_{0z} = 0.25$ taper ratio.

3.1.3. Square cross-section beams ($L_y/h_{0z} = 5$). For the case of beam with constant cross-section, results obtained using classical theories are erroneous. An error of

Downloaded from jvc.sagepub.com by Erasmo Carrera on August 26, 2014

Table 1. First ten frequencies (*rad./s*) for square cross-section beam; *a* – axial mode; *t* – torsional; EBBT – Euler-Bernoulli beam theory; TBT – Timoshenko beam theory.

		$L_y/h_{0z}=100$						$L_y/h_{0z}=10$						$L_y/h_{0z}=5$					
Taper (h_{fz}/h_{0z})	Mode	EBBT	TBT	$N=1$	$N=2$	$N=3$	ANSYS 3D	EBBT	TBT	$N=1$	$N=2$	$N=3$	ANSYS 3D	EBBT	TBT	$N=1$	$N=2$	$N=3$	ANSYS 3D
1.0	1	0.53	0.53	0.53	0.53	0.53	0.53	52.70	50.13	50.13	50.71	50.30	50.48	207.62	175.32	175.32	178.05	174.08	175.16
	2	0.53	0.53	0.53	0.53	0.53	0.53	52.70	50.13	50.13	50.71	50.30	50.48	207.63	175.32	175.32	178.05	174.08	175.16
	3	1.46	1.46	1.46	1.47	1.46	1.46	143.28	129.57	129.57	130.91	128.99	130.03	515.32^a	407.35	319.59^t	319.59^t	319.59^t	303.14^t
	4	1.46	1.46	1.46	1.47	1.46	1.46	143.31	129.57	129.57	130.91	128.99	130.03	543.53	407.35	407.35	411.44	398.78	403.10
	5	2.86	2.86	2.86	2.88	2.86	2.86	257.66^a	236.07	159.79^t	159.79^t	159.79^t	151.08^t	543.66	515.31^a	407.35	411.45	398.78	403.10
	6	2.86	2.86	2.86	2.88	2.86	2.86	275.09	236.07	236.07	238.17	233.36	236.40	992.36	684.40	425.63^a	521.38^a	520.82^a	521.00^a
	7	4.73	4.71	4.71	4.75	4.71	4.73	275.35	257.65^a	236.07	238.18	233.36	236.40	993.23	684.40	639.18^t	639.18^t	639.18^t	606.97^t
	8	4.74	4.72	4.72	4.76	4.72	4.73	442.52	361.00	259.29^a	259.41^a	259.33^a	259.49^a	1030.64^a	983.04	684.40	688.80	665.63	674.87
	9	7.06	7.03	7.03	7.09	7.06	7.07	443.61	361.02	319.59^t	319.59^t	319.59^t	302.44^t	1508.82	983.05	684.40	688.81	665.63	674.87
	10	7.10	7.06	7.06	7.12	7.06	7.07	515.32	498.79	361.02	363.74	354.79	361.21	1512.28	1030.62^a	958.76^t	958.76^t	958.76^t	912.19^t
0.5	1	0.39	0.39	0.39	0.39	0.39	0.39	38.66	37.60	37.60	38.07	37.86	37.91	153.32	138.66	138.66	141.09	138.97	139.38
	2	0.53	0.53	0.53	0.53	0.53	0.53	52.28	49.72	49.72	50.23	49.79	49.96	206.01	173.82	173.82	176.03	172.01	173.13
	3	1.07	1.07	1.07	1.07	1.07	1.07	105.64	99.67	99.67	100.84	99.84	100.42	410.12	339.99	321.80^t	307.88^t	306.83^t	291.68^t
	4	1.45	1.45	1.45	1.46	1.46	1.46	142.78	129.04	129.04	130.19	128.23	129.27	512.39^a	405.47	339.99	344.57	336.22	339.11
	5	2.09	2.09	2.09	2.10	2.10	2.09	204.60	186.49	160.93^t	152.44^t	152.21^t	144.25^t	541.69	512.38^a	405.47	408.69	395.93	400.36
	6	2.85	2.85	2.85	2.88	2.87	2.86	256.19^a	235.55	186.49	188.53	185.82	187.93	770.41	592.58	422.16^a	517.14^a	516.66^a	517.08^a
	7	3.45	3.45	3.45	3.47	3.47	3.46	274.84	256.19^a	209.30	237.33	232.47	235.50	991.43	682.69	592.58	598.69	580.94	581.58^t
	8	4.72	4.72	4.72	4.76	4.75	4.73	332.93	292.54	235.55^a	257.62^a	257.54^a	257.79^a	1029.26^a	874.36	639.98^t	613.47^t	610.84^t	588.65
	9	5.15	5.15	5.15	5.18	5.18	5.17	443.16	360.53	292.54^t	295.54^t	290.05^t	287.35^t	1207.85	981.65	682.69	685.96	662.64	672.07
	10	7.06	7.06	7.06	7.23	7.11	7.06	514.63	413.42	320.05	303.46	302.88	295.15	1545.23	1029.24^a	874.53^t	881.41	852.68	867.56^t
0.25	1	0.30	0.30	0.30	0.31	0.30	0.30	30.32	29.79	29.79	30.21	30.06	29.87	120.58	112.90	112.90	115.10	113.71	113.25
	2	0.51	0.51	0.51	0.52	0.51	0.51	51.21	48.66	48.66	49.13	48.66	48.77	201.83	169.88	169.88	171.73	167.62	168.63
	3	0.83	0.83	0.83	0.84	0.83	0.83	82.77	79.72	79.72	80.80	80.14	80.10	324.77	285.25	285.25^t	287.44	284.05	271.91^t
	4	1.44	1.44	1.44	1.45	1.44	1.44	141.33	127.58	127.58	128.63	126.61	127.50	504.63^a	400.19	323.75	290.01	285.18^t	285.04
	5	1.63	1.63	1.63	1.65	1.63	1.62	160.59	151.03	151.03^t	140.22^t	139.73^t	132.87^t	536.32	504.62^a	400.19	402.73	389.83	394.12
	6	2.68	2.68	2.68	2.72	2.68	2.68	252.32^a	234.02	161.94	153.07	151.27	152.29	617.69	510.11	415.38^a	507.91^a	503.58	508.23^a
	7	2.84	2.84	2.84	2.86	2.84	2.84	262.20	240.18	206.09	235.63	230.66	233.48	983.37	677.68	510.11	517.49	507.34^a	508.92
	8	4.00	3.99	3.99	4.06	3.99	4.00	273.38	252.31^a	234.02	243.45	239.63	243.36	986.35	768.81	640.19	560.99	555.06^t	531.14^t
	9	4.72	4.70	4.70	4.74	4.70	4.70	385.82	343.96	240.18^a	253.45^a	253.34^a	253.62^a	1025.03	977.41	677.68	679.98	656.48	665.78
	10	5.56	5.55	5.55	5.64	5.55	5.59	441.83	359.06	320.22	271.85^t	270.57^t	258.07^t	1405.68	1050.42	841.17	778.60	754.38	767.44

Downloaded from jvc.sagepub.com by Erasmo Carrera on August 26, 2014

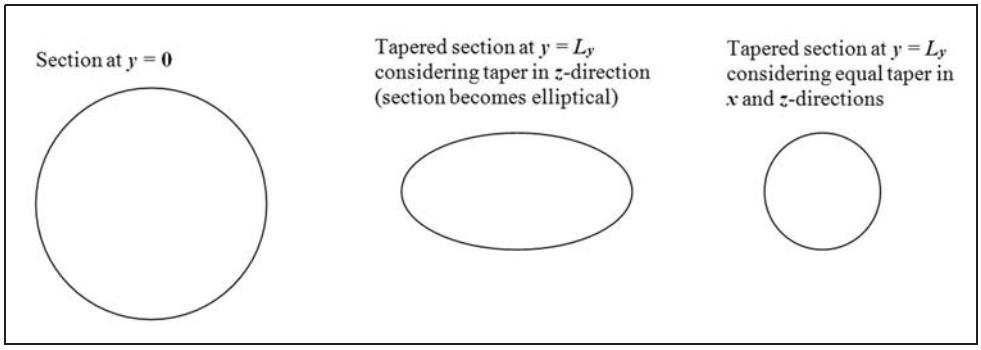

Figure 2. Section view of different tapering schemes considered for circular cross-section beam.

Table 2. First ten frequencies (*rad./s*) for circular cross-section beam ($L_y/h_{0z} = 10$).

	Uniform beam ($h_{fz}/h_{0z} = 1.0$)		Taper in one direction (h_{fz}/h_{0z})		Equal taper in two directions (h_{fz}/h_{0z} and h_{fx}/h_{0x})	
Mode	$N = 3$	ANSYS 3D	0.5	0.25	0.5	0.25
1	44.24	43.84	33.04	26.14	33.24	26.77
2	44.24	43.84	43.85	42.90	33.24	26.77
3	115.42	114.92	88.07	70.17	88.25	70.83
4	115.42	114.92	114.91	113.58	88.25	70.83
5	159.79^t	159.28^t	151.77^t	133.47	165.90	134.09
6	212.30	212.49	165.80	138.68^t	165.90	134.09
7	212.30	212.49	211.83	210.39	166.48^t	183.24^t
8	259.17^a	259.31^a	257.45^a	213.20	258.32^a	209.41^a
9	319.59^t	318.81^t	261.81	253.33^a	261.86	214.37
10	327.52	329.74	301.89^t	268.00^t	261.86	214.37

a – axial mode; *t* – torsional.

about 18% is seen for the vibration frequencies of bending modes obtained using EBBT when compared with that obtained using refined theory with $N = 3$ and ANSYS 3D. For the case of the beam with $h_{fz}/h_{0z} = 0.5$, there is a decrease in vibration frequencies of about 15–20%, 5% and 1% for bending, torsional and axial modes respectively. It is 30%, 10–13%, and 2.5% for bending, torsional and axial modes respectively for $h_{fz}/h_{0z} = 0.25$. Also, there is a decrease of about 2% in the vibration frequencies in the un-tapered direction for the case of $h_{fz}/h_{0z} = 0.25$.

The aspect ratio (L_y/h_{0z}) significantly affects the vibration characteristics. Considering the cases of beams with $L_y/h_{0z} = 10$ and 5, it is observed for a beam with $L_y/h_{0z} = 5$, frequencies of bending modes become more than three times of that of the corresponding frequencies of beams with $L_y/h_{0z} = 10$ whereas in the case of torsional and axial modes, the frequencies become twice.

3.1.4. Circular cross-section beams ($L_y/h_{0z} = 10$). A clamped supported circular cross-section beam with $L_y/h_{0z} = 10$ is considered. Results are presented for constant cross-section beam as well as for the beams two tapering ratios ($h_{fz}/h_{0z} = 0.5$ and 0.25). Tapering in both the cross-sectional direction is also considered as shown in Figure 2. All the results are obtained using refined theory with expansion order $N = 3$ and presented in Table 2. It can be observed from Table 2 that for the case of $h_{fz}/h_{0z} = 0.5$ in only one direction, frequency decreases by 20–25% for bending modes, 5–6% for torsional and there is almost negligible change in axial modes. The change is more apparent in the first bending modes. For $h_{fz}/h_{0z} = 0.25$, the change is 35–40%, 12–16% and 2% for bending, torsional and axial modes, respectively. For the case of taper in both directions, it is interesting to observe that the vibration frequency of torsional mode is not only higher than that of the corresponding mode of beam with one side taper but also higher than that of the untapered beam. This is due to the formation of an elliptic section at the tapered end of the beams with one side taper which results in a reduction of its torsional rigidity. In the case of taper in both directions,

Downloaded from jvc.sagepub.com by Erasmo Carrera on August 26, 2014

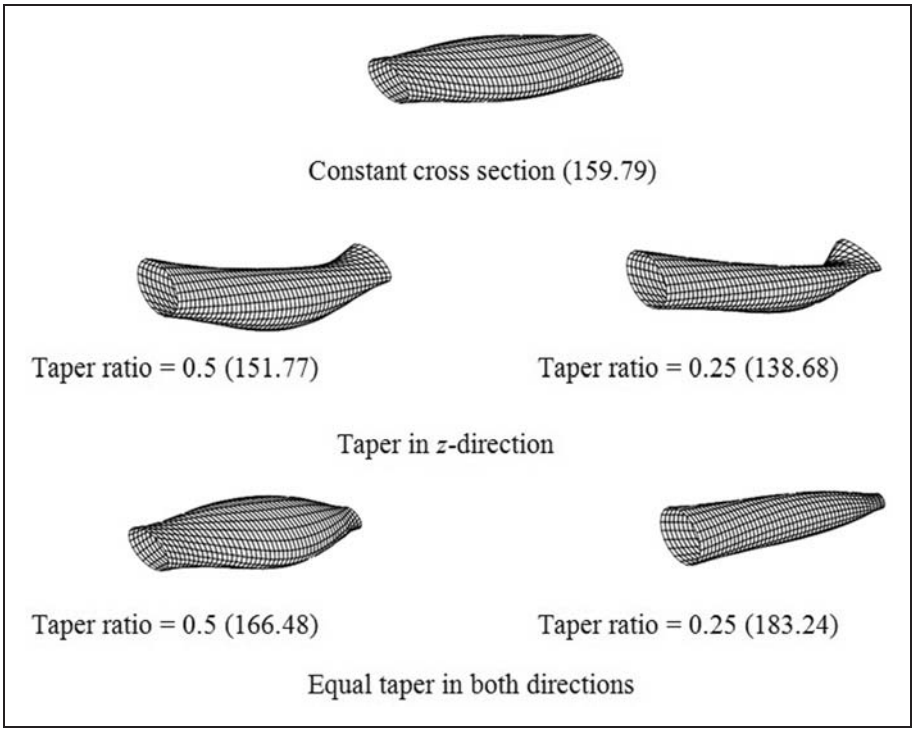

Figure 3. First torsional modes of solid circular cross-section beams with different taper ratios for $N = 3$ (Frequencies in rad./s written within brackets).

the increase in fundamental torsional frequency is mainly due to the change in the distribution of mass and stiffness along the length of the beam. It may be noted here that the mass density of the material was kept uniform and thus the total mass of beams varies with the change in its cross-section. For clarity, torsional modes for different taper ratios are plotted in Figure 3.

3.2. Rectangular plates

In this section, natural frequencies of vibrating plates are discussed which are expressed in terms of the frequency factor $\lambda = \omega L_x^2(\rho h_{0z}/d_0)^{1/2}/\pi^2$, where ω is the natural frequency, L_x is the length of the plate along x-axis; h_{0z} is the initial thickness and $d_0 = Eh_0^3/\left(12\left(1-\upsilon^2\right)\right)$. The first ten frequency factor values are given for each case based on the different theories and are compared with ANSYS 3D (total dof = 2583) and published results.

For validation purposes, cantilevered plates having aspect ratio (L_y/L_x) of 2.0 and taper ratio (h_{fz}/h_{0z}; where h_{fz} is the thickness of plate at $y = L_y$) as 0.5 with two different thickness ratios ($h_{0z}/L_x = 0.1$ and 0.3) are considered and the first ten frequency factors along with the mode types (a – axial modes; z – bending along z-axis; t – bending modes in both x- and y-axes) are given in Table 3. Present results are confirmed with ANSYS 3D solutions and with the only available results of vibrating tapered plate analysis carried out using higher order theory by Shufrin and Eisenberger (2006). Because of the displacement field considered along three axes, even the results obtained using classical theories predict inplane modes (a – axial modes; z – bending modes in z axis). However, twisting type modes come in to the picture only with theory expansion order $N > 1$. It can be seen that results obtained using $N = 3$ gives comparable results with that of obtained using ANSYS 3D as well as with published results for both thickness ratios. It is apt to mention here that because of the 2D nature of higher order theory used by Shufrin and Eisenberger (2006), bending modes along z-axis and purely axial modes (e.g. mode 7 in Table 3 for $h_{0z}/L_x = 0.3$), are missed in their study. It is also observed from Table 3 that by increasing the thickness of plates, vibrating frequencies get reduced. The first ten modes, for $h_{0z}/L_x = 0.1$ and 0.3 are plotted in Figures 4 and 5, respectively.

Results are also given in Table 4 for plates with two free and other two parallel edges clamped for $h_{0z}/h_{fz} = 0.5$ and $L_y/L_x = 2.0$. It can be seen from Table 4 that frequency values match very well with ANSYS 3D results. It can be observed that inplane modes come up earlier as compared to that of the previous case. Also, except for the first few modes, it can be seen that

Downloaded from jvc.sagepub.com by Erasmo Carrera on August 26, 2014

Table 3. First ten frequency factors λ for cantilever taper plates with thickness variation in the y direction for different theories ($L_y/L_x = 2.0$, $h_{fz}/h_{0z} = 0.5$).

h_{0z}/L_x	Mode	EBBT	TBT	$N=1$	$N=2$	$N=3$	$N=4$	ANSYS 3D	Ref.* (HOPT)
0.1	1	0.0920	0.0919	0.0919	0.0953	0.0942	0.0939	0.0943	0.0961
	2	0.4398	0.4374	0.4374	0.3371^t	0.3325^t	0.3297^t	0.3275^t	0.3262
	3	0.9860^z	0.8846^z	0.8846^z	0.4542	0.4477	0.4463	0.4491	0.4560
	4	1.1319	1.1180	1.1180	0.8911^z	0.8764^z	0.8750^z	0.8742^z	–
	5	2.1588	2.1125	1.8629^t	0.9176^t	0.8783^t	0.8783^t	0.8767^t	0.8758
	6	2.9997^a	2.9997^a	2.1125	1.1681	1.1445	1.1399	1.1502	1.1607
	7	3.5173	3.0869^z	2.4543^a	1.7673^t	1.6751^t	1.5338^t	1.4956^t	1.4899
	8	4.3819^z	3.4029	3.0869^z	2.2043	1.7535^a	1.6562^a	1.6551^a	1.6558
	9	5.2000	4.9654	3.4029	2.5770^a	2.1939	2.1697	2.1849	2.2177
	10	7.1981	6.2019^z	4.9654	2.9270^t	2.5553^a	2.3439^a	2.2608^a	3.0957
0.3	1	0.0918	0.0909	0.0909	0.0929	0.0927	0.0924	0.0929	0.0941
	2	0.3287^z	0.2949^z	0.2949^z	0.2977^z	0.2925^z	0.2920^z	0.2927^z	–
	3	0.4344	0.4150	0.4150	0.3150^t	0.3109^t	0.2997^t	0.2985^t	0.2980
	4	0.9999^a	0.9999^a	0.6275^t	0.4244	0.4205	0.4193	0.4229	0.4261
	5	1.0987	1.0009	0.8202^a	0.8220^t	0.7981^t	0.7722^t	0.7714^t	0.7731
	6	1.4606^z	1.0290^z	1.0009	1.0063^a	1.0004^z	0.9972^z	0.9994^z	–
	7	2.0442	1.7677	1.0290^z	1.0244	1.0052^a	1.0019^a	1.0069^a	–
	8	2.6759^a	2.0673^z	1.6622^t	1.0314^z	1.0059	1.0046	1.0133	1.0163
	9	3.1745^z	2.6591	1.7677	1.4924^t	1.4252^a	1.3637^a	1.3340^a	1.3299
	10	3.2302	2.6758^a	2.0673^z	1.6484^a	1.5616^t	1.3814^t	1.3860^t	1.3871

*- Shufrin and Eisenberger (2006), HOPT – Higher order plate theory.
EBBT – Euler Bernoulli beam theory; TBT – Timoshenko beam theory.
a – axial mode; t – biaxial bending; z-bending in z-axis.

different types of modes appear in a narrow band of frequency.

A parametric study pertaining to the effects of L_y/L_x, h_{fz}/h_{0z} and h_{0z}/L_x on free vibration frequencies has also been carried out and the results for different parameters are presented in Table 5. It can be observed from Table 5 that due to the increased flexibility of plates having a bigger aspect ratio, the influence of thickness variation gets reduced. As a result of an increase in plate thickness, the number of axial as well as bending modes in z-axis increases.

It can be noted that the frequencies of torsional modes for beams and plates predicted by higher order theory ($N \geq 3$) are slightly on the higher side as compared with those obtained using ANSYS. This slight overestimation of frequencies of non-classical modes can be attributed to the slow convergence of the numerical algorithm used.

4. Conclusions

Free vibrations of beams and plates with variable thickness using an efficient unified theory have been investigated on a unified basis wherein results are presented in the form of Euler-Bernoulli/Timoshenko to quasi 3D solutions. Modes like bending, torsional, biaxial bending as well different kinds of inplane modes are captured which are in very good agreement with 3D finite element results as well as the published literature. The main conclusions drawn from the present analysis are:

- Due to taper, bending vibration modes become asymmetric along the longitudinal axis of the structure.
- The effect of taper is more pronounced in bending modes as compared to that of axial and torsional modes.
- Because of the formation of an elliptical cross-section in the case of circular beams with one side taper or unequal taper in the two transverse directions, the torsional rigidity becomes comparatively less than that in the case with uniform taper in both directions.
- The taper of beams of a circular section in one direction makes the section elliptical at one end thus

Downloaded from jvc.sagepub.com by Erasmo Carrera on August 26, 2014

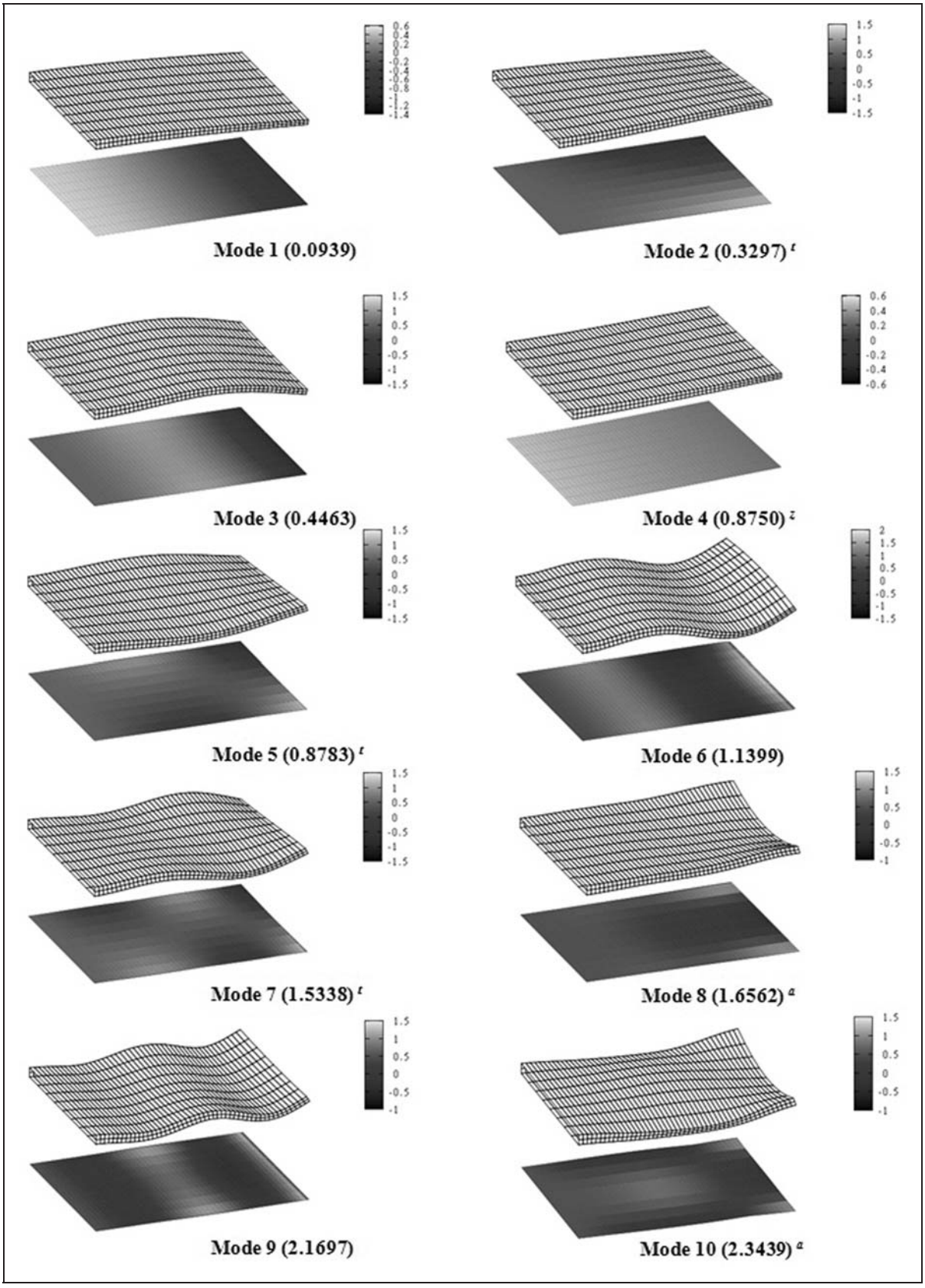

Figure 4. First ten mode shapes along with frequency factors λ of solid cantilever tapered plate with $h_0/L_x = 0.1$ for $N = 4$ (a – axial mode; t – biaxial bending; z – bending in z-axis).

Downloaded from jvc.sagepub.com by Erasmo Carrera on August 26, 2014

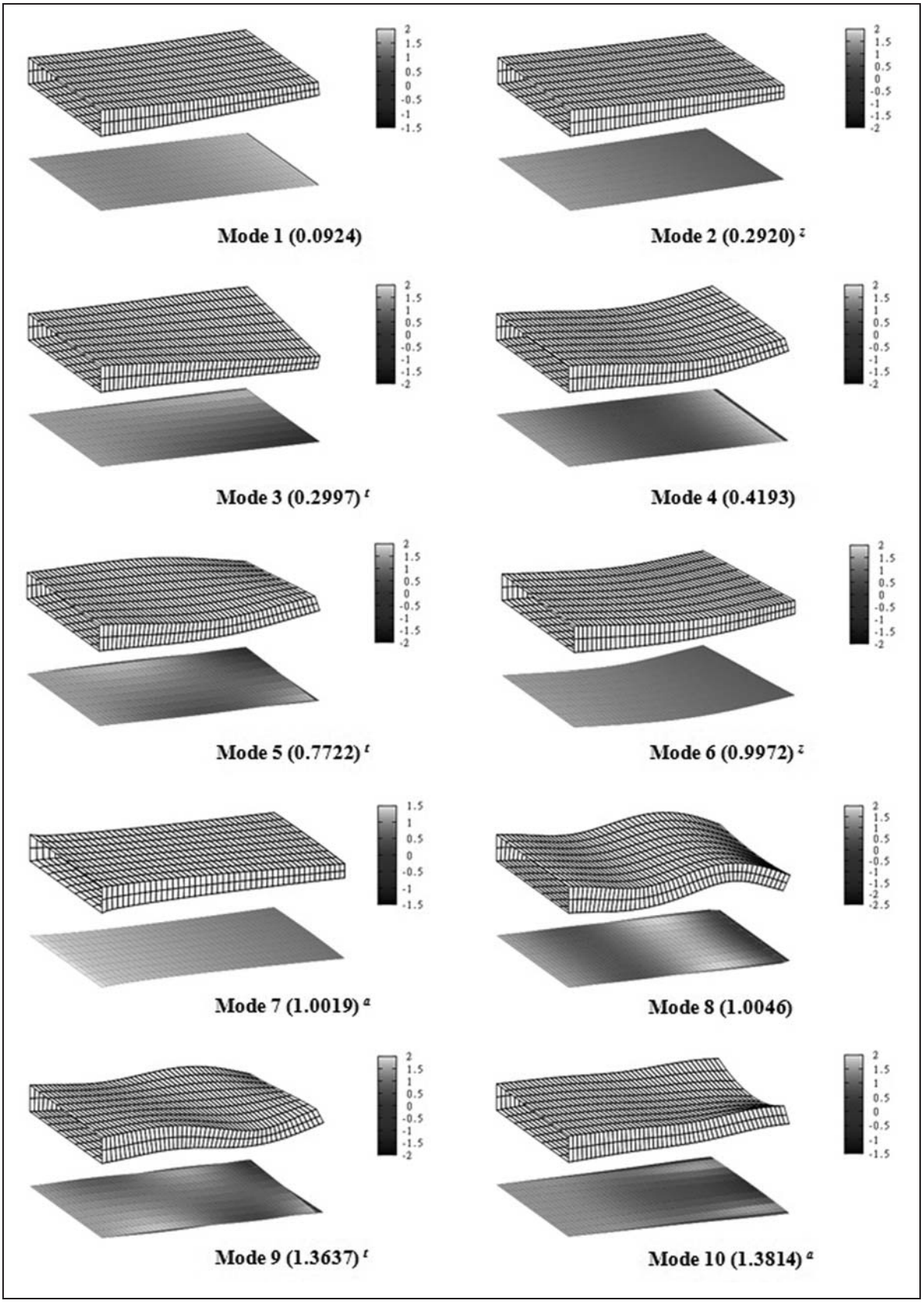

Figure 5. First ten mode shapes along with frequency factors λ of solid cantilever tapered plate with $h_0/L_x = 0.3$ for $N = 4$ (a – axial mode; t – biaxial bending; z – bending in z-axis).

Downloaded from jvc.sagepub.com by Erasmo Carrera on August 26, 2014

Table 4. First ten frequency factors λ for two free and other two parallel edges clamped taper plates with thickness variation in *y* direction for different theories ($L_y/L_x = 2.0$, $h_{fz}/h_{0z} = 0.5$).

h_{0z}/L_x	Mode	EBBT	TBT	$N=1$	$N=2$	$N=3$	$N=4$	ANSYS 3D
0.1	1	0.3954	0.3926	0.3926	0.4121	0.4079	0.4063	0.4059
	2	1.0866	1.0698	1.0698	0.6928^t	0.6659^t	0.6621^t	0.6562^t
	3	2.1225	2.0678	2.0678	1.1229	1.1103	1.1057	1.1099
	4	3.4932	2.7489^a	2.7489^z	1.5832^t	1.4985^t	1.4908^t	1.4828^t
	5	4.7822^z	3.3606	3.2439^t	2.1700	2.1457	2.0039	1.9472
	6	5.1909	4.9232	3.3606	2.7636^z	2.2483^a	2.1374^a	2.1592^a
	7	5.2294^a	5.2293^a	4.3369^a	2.7714^t	2.5958^t	2.5807^t	2.5823^t
	8	7.2060	5.3981^z	4.9232	3.5237	2.6528^z	2.6398^z	2.6371^z
	9	9.5255	6.7295	5.3981^z	3.8145^a	3.1503^a	2.9477^a	2.8213^a
	10	10.5046^a	8.6385^z	6.5150^t	4.2598^t	3.4864	3.4702	3.5335
0.3	1	0.3931	0.3703	0.3703	0.3839	0.3795	0.3779	0.3787
	2	1.0646	0.9163^z	0.9163^z	0.6131^t	0.5931^t	0.5746^t	0.5719^t
	3	1.5941^z	0.9455	0.9455	0.9223^z	0.8850^z	0.8804^z	0.8799^z
	4	1.7431^a	1.7041	1.0832^t	0.9767	0.9581	0.9542	0.9610
	5	2.0344	1.7431^a	1.4517^a	1.3194^t	1.2655^t	1.2278^t	1.2266^t
	6	3.2548	1.7994^z	1.7041	1.7549	1.7121	1.6812	1.6414
	7	3.5015^a	2.5824	1.7994^z	1.7653^a	1.7441^z	1.7079^z	1.7274^z
	8	3.5256^z	2.8795^z	2.1724^t	1.8004^z	1.7619^a	1.7343^a	1.7341^a
	9	4.6787	3.0813^z	2.5824	2.0335^a	1.9051^a	1.7600^a	1.7618^a
	10	5.2569^a	3.5015^a	2.8760^a	2.1511^t	2.0543^t	1.9920^t	2.0001^t

a – axial mode; *t* – biaxial bending; *z* – bending in z-axis.
EBBT – Euler Bernoulli beam theory; TBT – Timoshenko beam theory.

Table 5. First ten frequency factors λ for two free and other two parallel edges clamped taper plates with thickness variation in *y* direction for different L_y/L_x, h_{0z}/h_{fz}, and h_{0z}/L_x ($N=4$).

			λ									
L_y/L_x	h_{0z}/h_{fz}	h_{0z}/L_x	1	2	3	4	5	6	7	8	9	10
1	0.5	0.1	1.5977	1.9041^t	3.3986^a	4.2105	4.6404^t	5.9902^z	6.4093^t	7.8262	8.3332^t	9.1636^a
		0.3	1.2805	1.4974^t	1.9967^z	2.5471^a	2.8596	3.1864^t	3.5427^a	3.6513^z	3.9328^t	4.1746^a
	0.25	0.1	1.2696	1.5355^t	2.7613^a	3.3847	3.7356^t	5.2294^a	5.8642^z	6.3775	6.7898^t	8.4542^a
		0.3	1.0889	1.2929^t	1.9510^z	2.2329^a	2.5306	2.8123^t	3.4666^a	3.5878^z	3.7513^a	3.9163^a
1.5	0.5	0.1	0.7221	1.0059^t	1.9479	2.3574^t	2.5522^a	3.7223	3.7690^z	4.0373^a	4.1864^t	5.9614
		0.3	0.6422	0.8630^t	1.2571^z	1.5497	1.8608^t	2.0871^a	2.3534^a	2.3967^z	2.6769	2.9850^a
	0.25	0.1	0.5697	0.8125^t	1.5410	1.8763^t	2.0225^a	2.9652	3.2646^a	3.3449^t	3.6833^z	4.7866
		0.3	0.5262	0.7295^t	1.2268^z	1.3111	1.5821^t	1.7616^a	2.3102^a	2.3230	2.3589^z	2.6153^a
2	0.5	0.1	0.4063	0.6621^t	1.1057	1.4908^t	2.0039	2.1374^a	2.5807^t	2.6398^z	2.9477^a	3.4702
		0.3	0.3779	0.5746^t	0.8804^z	0.9542	1.2278^t	1.6812	1.7079^z	1.7343^a	1.7600^a	1.9920^t
	0.25	0.1	0.3208	0.5393^t	0.8739	1.1880^t	1.6892	1.7307^a	2.0577^t	2.5361^z	2.5902^a	2.7660
		0.3	0.3054	0.4974^t	0.7898	0.8632^z	1.0542^t	1.4424	1.5534^a	1.7176^z	1.7314^a	1.7397^t

a – axial mode; *t* – biaxial bending; *z* – bending in z-axis.

Downloaded from jvc.sagepub.com by Erasmo Carrera on August 26, 2014

reducing its torisional rigidity which results in a decrease in the fundamental torsional frequency. Whereas, both side taper results in the increase in the fundamental torsional frequency which is mainly due to the change in the distribution of mass and stiffness along the length of beam.

- The presence of axial modes is quite significant in the first ten modes of thicker beams and plates as compared to that of relatively thinner beams/plates.
- The use of unified theory is recommended for the analysis of shorter beams and thick plates with taper.

Acknowledgements

The authors are grateful for the financial support received from the Deanship of Scientific Research at King Saud University. Thanks are also extended to the MMB Chair for Research and Studies in Strengthening and Rehabilitation of Structures, at the Department of Civil Engineering, King Saud University for providing technical support.

Funding

This work was supported by the Deanship of Scientific Research at King Saud University (grant number RGP-VPP-104).

References

Al-Kaabi SA and Aksu G (1987) Free vibration analysis of Mindlin plates with linearly varying thickness. *Journal of Sound and Vibration* 119: 189–205.

Al-Kaabi SA and Aksu G (1988) Natural frequencies of Mindlin plates of bilinearly varying thickness. *Journal of Sound and Vibration* 123: 373–379.

Al-Kaabi SA and Aksu G (1990) Free vibration analysis of Mindlin plates with parabolically varying thickness. *Computers and Structures* 34: 395–399.

Attarnejad R, Semnani SJ and Shahba A (2010) Basic displacement functions for free vibration analysis of non-prismatic Timoshenko beams. *Finite Elements in Analysis and Design* 10: 916–929.

Auciello NM and Ercolano A (2004) A general solution for dynamic response of axially loaded non-uniform Timoshenko beams. *International Journal of Solids and Structures* 41: 4861–4874.

Bathe KJ (1996) *Finite Element Procedure*. Upper Saddle River, NJ: Prentice Hall.

Carrera E and Brischetto S (2008) Analysis of thickness locking in classical, refined and mixed multilayered plate theories. *Composite Structures* 82: 549–62.

Carrera E and Petrolo M (2012) Refined beam elements with only displacement variables and plate/shell capabilities. *Meccanica* 47: 537–556.

Carrera E, Giunta G and Petrolo M (2011) *Beam Structures: Classical and Advanced Theories*. West Sussex, UK: John Wiley & Sons.

Cheung YK and Zhou D (2003) Vibration of tapered Mindlin plates in terms of static Timoshenko beam functions. *Journal of Sound and Vibration* 260: 693–709.

Dawe DJ and Wang S (1994) Vibration of shear-deformable beams, plates using spline representations of deflection, shear strains. *International Journal of Mechanical Sciences* 36: 469–481.

Doong JL (1987) Vibration and stability of an initially stressed thick plate according to a higher order deformation theory. *Journal of Sound and Vibration* 113: 425–440.

Gupta AK and Sharma P (2011) Thermally induced vibration of orthotropic trapezoidal plate of linearly varying thickness. *Journal of Vibration and Control* 17(10): 1591–1598.

Gupta AK and Sharma P (2012) Effect of linear thermal gradient on vibrations of trapezoidal plates whose thickness varies parabolically. *Journal of Vibration and Control* 18(3): 395–403.

Hajianmaleki M and Qatu MS (2012) Static and vibration analysis of thick generally laminated deep curved beams with different boundary conditions. *Composites Part B: Engineering* 43: 1767–1775.

Hanna NF and Leissa AW (1994) A higher order shear deformation theory for the vibration of thick plates. *Journal of Sound and Vibration* 170: 545–555.

Kerr AD (1969) An extended Kantorovich method for the solution of eigenvalue problem. *International Journal of Solids and Structures* 15: 559–572.

Liew KM, Wang CM, Xiang Y and Kitipornchai S (1998) *Vibration of Mindlin Plates*. Amsterdam: Elsevier.

Malekzadeh P and Karami G (2004) Vibration of non-uniform thick plates on elastic foundation by differential quadrature method. *Engineering Structures* 26: 1473–1482.

Manna MC (2012) Free vibration of tapered isotropic rectangular plates. *Journal of Vibration and Control* 18(1): 76–91.

Matsunga H (1994) Free vibration and stability of thick elastic plates subjected to in-plane forces. *International Journal of Solids and Structures* 31: 3113–3124.

Mikami T and Yoshimura J (1984) Application of the collocation method to vibration analysis of rectangular Mindlin plates. *Computer & Structures* 18: 425–431.

Mizusawa T (1993) Vibration of rectangular Mindlin plates with tapered thickness by the spline strip method. *Computer & Structures* 44: 451–463.

Piovan MT, Filipich CP and Cortínez VH (2008) Exact solutions for coupled free vibrations of tapered shear-flexible thin-walled composite beams. *Journal of Sound and Vibration* 316: 298–316.

Quintana MV and Nallim LG (2010) A variational approach to free vibration analysis of shear deformable polygonal plates with variable thickness. *Applied Acoustics* 71: 393–401.

Downloaded from jvc.sagepub.com by Erasmo Carrera on August 26, 2014

Reddy JN and Phan ND (1985) Stability and vibration of isotropic, orthotropic and laminated plates according to a higher-order shear deformation theory. *Journal of Sound and Vibration* 98: 157–170.

Shufrin I and Eisenberger M (2005) Stability and vibration of shear deformable plates — first order and higher order analyses. *International Journal of Solids and Structures* 42: 1225–1251.

Shufrin I and Eisenberger M (2006) Vibration of shear deformable plates with variable thickness – first-order and higher-order analyses. *Journal of Sound and Vibration* 290: 465–489.

Tsai SW (1988) *Composites Design*. *Think Composites*, 4th edn. Ohio: Dayton.

Downloaded from jvc.sagepub.com by Erasmo Carrera on August 26, 2014